Mechanics and Mechanical Engineering
Vol. 21, No. 2 (2017) 267–289

Elastodynamic Problem for an Infinite Body Having a Spherical Cavity in the Theory of Thermoelasticity with Double Porosity

Rajneesh M. Kumar
Department of Mathematics
Kurukshetra University
Kurukshetra, Haryana,India
Rajneesh_kuk@rediffmail.com

Richa Vohra
Department of Mathematics and Statistics
H.P. University, Shimla, HP, India
richavhr88@gmail.com

Received (29 Januaryt 2017)
Revised (6 February 2017)
Accepted (11 March 2017)

The present investigation is concerned with homogeneous, isotropic infinite double porous thermoelastic body with a spherical cavity subjected to ramp type mechanical/thermal source in the context of Lord-Shulman theory of thermoelasticity [1] with one relaxation time. Laplace transform technique has been used to obtain the expressions for radial stress, hoop stress, equilibrated stresses and temperature distribution. A numerical inversion technique has been applied to recover the resulting quantities in the physical domain. The components of stress and temperature distribution are depicted graphically to show the effect of porosity and relaxation time parameters. Some particular cases are also deduced from the present investigation.

Keywords: double porosity, thermoelasticity, Lord–Shulman theory, spherical cavity.

1. Introduction

Porous media theories play an important role in many branches of engineering including material science, the petroleum industry, chemical engineering, biomechanics and other such fields of engineering. Biot [2] proposed a general theory of three-dimensional deformation of fluid saturated porous salts. One important generalization of Biot's theory of poroelasticity that has been studied extensively started with the works by Barenblatt et al. [3] where the double porosity model was first proposed to express the fluid flow in hydrocarbon reservoirs and aquifers. The double porosity model represents a new possibility for the study of important

problems concerning the civil engineering. It is well-known that, under super- saturation conditions due to water of other fluid effects, the so called neutral pressures generate unbearable stress states on the solid matrix and on the fracture faces, with severe (sometimes disastrous) instability effects like landslides, rock fall or soil fluidization (typical phenomenon connected with propagation of seismic waves). In such a context it seems possible, acting suitably on the boundary pressure state, to regulate the internal pressures in order to deactivate the noxious effects related to neutral pressures; finally, a further but connected positive effect could be lightening of the solid matrix/fluid system

Aifantis [4–7] introduced a multi–porous system and studied the mechanics of diffusion in solids. Wilson and Aifanits [8] presented the theory of consolidation with the double porosity. Khaled et. al [9] employed a finite element method to consider the numerical solutions of the differential equation of the theory of consolidation with double porosity developed by Wilson and Aifantis [8]. Wilson and Aifantis [10] discussed the propagation of acoustics waves in a fluid saturated porous medium. The propagation of acoustic waves in a fluid–saturated porous medium containing a continuously distributed system of fractures is discussed.

Nunziato and Cowin [11] developed a nonlinear theory of elastic material with voids. Later, Cowin and Nunziato [12] developed a theory of linear elastic materials with voids for the mathematical study of the mechanical behavior of porous solids. They also considered several applications of the linear theory by investigating the response of the materials to homogeneous deformations, pure bending of beams and small amplitudes of acoustic waves. Nunziato and Cowin have established a theory for the behavior of porous solids in which the skeletal or matrix materials are elastic and the interstices are voids of material.

Beskos and Aifantis [13] presented the theory of consolidation with double porosity-II and obtained the analytical solutions to two boundary value problems. Khalili and Valliappan [14] studied the unified theory of flow and deformation in double porous media. Khalili and Selvadurai [15] presented a fully coupled constitutive model for thermo–hydro–mechanical analysis in elastic media with double porosity structure. Various authors [16–21] investigated some problems on elastic solids, viscoelastic solids and thermoelastic solids with double porosity.

Iesan and Quintanilla [22] used the Nunziato-Cowin theory of materials with voids to derive a theory of thermoelastic solids, which have a double porosity structure. This theory is not based on Darcy's law. In contrast with the classical theory of elastic materials with the double porosity, the double porosity structure in the case of equilibrium is influenced by the displacement field.

Allam et al. [23] studied the thermal stresses in a harmonic field for an infinite body with a circular cylindrical hole without energy dissipation. Youseff [24] investigated the problem of infinite body with a cylindrical cavity and variable material properties in generalized thermoelasticity.Youseff [25] studied the problem of an infinite material with a spherical cavity and variable thermal conductivity subjected to ramp–type heating. Allam et al [26] considered the model of generalized thermoelasticity proposed by Green and Naghdi, to study the electromagneto–thermoelastic interactions in an infinite perfectly conducting body with a spherical cavity. Abd–Alla and Abo–Dahab [27] investigated the effect of rotation and initial stress on an infinite generalized magneto–thermoelastic diffusion body with a spherical cavity.

Zenkour and Abouelregal [28] studied the effects of phase–lags in a thermoviscoelastic orthotropic continuum with a cylindrical hole and variable thermal conductivity. Abbas et al. [29] investigated the thermoelastic interactions in a thermally conducting cubic crystal subjected to ramp-type heating.

The present paper deals with elastodynamic deformation in an infinite double porous thermoelastic body with a spherical cavity subjected to ramp type mechanical/thermal source in the context of Lord-Shulman theory of thermoelasticity. Laplace transform has been applied to find the expressions for the components of stress and temperature distribution. The resulting quantities are obtained in the physical domain by using a numerical inversion technique. Variation of radial stress, hoop stress, equilibrated stresses and temperature distribution against radial distance are depicted graphically to show the effect of porosity and thermal relaxation time. Some special cases of interest have also been deduced from the present investigation.

2. Basic equations

Following Iesan and Quintanilla [22] and Lord and Shulman [1]; the constitutive relations and field equations for homogeneous isotropic thermoelastic material with double porosity structure in the absence of body forces, extrinsic equilibrated body forces and heat sources can be written as:
Constitutive Relations:

$$t_{ij} = \lambda e_{rr}\delta_{ij} + 2\mu e_{ij} + b\delta_{ij}\varphi + d\delta_{ij}\psi - \beta\delta_{ij}T \tag{1}$$

$$\sigma_i = \alpha\varphi_{,i} + b_1\psi_{,i} \tag{2}$$

$$\chi_i = b_1\varphi_{,i} + \gamma\psi_{,i} \tag{3}$$

Equation of motion:

$$\mu\nabla^2 u_i + (\lambda+\mu)\, u_{j,ji} + b\varphi_{,i} + d\psi_{,i} - \beta T_{,i} = \rho\ddot{u}_i, \tag{4}$$

Equilibrated stress equations of motion:

$$\alpha\nabla^2\varphi + b_1\nabla^2\psi - bu_{r,r} - \alpha_1\varphi - \alpha_3\psi + \gamma_1 T = \kappa_1\ddot{\varphi}, \tag{5}$$

$$b_1\nabla^2\varphi + \gamma\nabla^2\psi - du_{r,r} - \alpha_3\varphi - \alpha_2\psi + \gamma_2 T = \kappa_2\ddot{\psi}, \tag{6}$$

Equation of heat conduction:

$$\left(1 + \tau_0\frac{\partial}{\partial t}\right)\left(\beta T_0\dot{u}_{j,j} + \gamma_1 T_0\dot{\varphi} + \gamma_2 T_0\dot{\psi} + \rho C^*\dot{T}\right) = K^*\nabla^2 T \tag{7}$$

where: λ and μ are Lame's constants, ρ is the mass density, $\beta = (3\lambda + 2\mu)\,\alpha_t$, α_t is the linear thermal expansion; C^* is the specific heat at constant strain, u_i is the displacement components, t_{ij} is the stress tensor, κ_1 and κ_2 are coefficients of equilibrated inertia, σ_i is the components of the equilibrated stress vector associated to pores, χ_i is the components of the equilibrated stress vector associated to fissures,

φ is the volume fraction field corresponding to pores and ψ is the volume fraction field corresponding to fissures, K^* is the coefficient of thermal conductivity, τ_0 is the thermal relaxation time, κ_1 and κ_2 are coefficients of equilibrated inertia and b, d, b_1, γ, γ_1, γ_2 are constitutive coefficients, δ_{ij} is the Kronecker's delta; T is the temperature change measured form the absolute temperature T_0 $(T_0 \neq 0)$, a superposed dot represents differentiation with respect to time variable t.

3. Formulation of the problem

We consider a homogeneous, isotropic thermoelastic infinite body having double porosity structure with a spherical cavity of radius a. The spherical polar coordinates $(r, \vartheta, \phi)$are taken for any representative point of the body at time t and the origin of the coordinate system is at the centre of the spherical cavity. All the variables considered will be functions of the radial distance r and the time t.
Due to spherical symmetry, the displacements components are of the form:

$$u_r = u(r,t) \qquad u_\vartheta = u_\phi = 0 \tag{8}$$

The components of stress for a spherical symmetric system become:

$$t_{rr} = 2\mu\frac{\partial u}{\partial r} + \lambda e + b\varphi + d\psi - \beta T \tag{9}$$

$$t_{\vartheta\vartheta} = t_{\phi\phi} = 2\mu\frac{u}{r} + \lambda e + b\varphi + d\psi - \beta T \tag{10}$$

$$t_{r\vartheta} = t_{r\phi} = t_{\vartheta\phi} = 0 \tag{11}$$

$$\sigma_r = \alpha\frac{\partial\varphi}{\partial r} + b_1\frac{\partial\psi}{\partial r} \tag{12}$$

$$\chi_r = b_1\frac{\partial\varphi}{\partial r} + \gamma\frac{\partial\psi}{\partial r} \tag{13}$$

where:

$$e = e_{rr} + e_{\vartheta\vartheta} + e_{\phi\phi} = \frac{\partial u}{\partial r} + \frac{2u}{r} \tag{14}$$

$$e_{rr} = \frac{\partial u}{\partial r} \qquad e_{\vartheta\vartheta} = e_{\phi\phi} = \frac{u}{r} \qquad e_{r\vartheta} = e_{r\phi} = e_{\vartheta\phi} = 0$$

We introduce the non-dimensional quantities as:

$$r' = \frac{\omega_1}{c_1}r \qquad u' = \frac{\omega_1}{c_1}u \qquad t'_{ij} = \frac{t_{ij}}{\beta T_0} \qquad \varphi' = \frac{\kappa_1\omega_1^2}{\alpha_1}\varphi \qquad \psi' = \frac{\kappa_1\omega_1^2}{\alpha_1}$$

$$T' = \frac{T}{T_0} \qquad t' = \omega_1 t \qquad \sigma'_i = \left(\frac{c_1}{\alpha\omega_1}\right)\sigma_i \qquad \chi'_i = \left(\frac{c_1}{\alpha\omega_1}\right)\chi_i \qquad \tau'_0 = \omega_1\tau_0 \tag{15}$$

where: $c_1^2 = \frac{\lambda+2\mu}{\rho}$, $\omega_1 = \frac{\rho C^* c_1^2}{K^*}$
Making use of dimensionless quantities given by (15) on Eqs.(4)–(7) and with the aid of Eq.(14) yield (dropping primes for convenience):

$$\frac{\partial e}{\partial r} + a_1\frac{\partial\varphi}{\partial r} + a_2\frac{\partial\psi}{\partial r} - a_3\frac{\partial T}{\partial r} = \frac{\partial^2 u}{\partial t^2} \tag{16}$$

$$a_4\nabla^2\varphi + a_5\nabla^2\psi - a_6 e - a_7\varphi - a_8\psi + a_9 T = \frac{\partial^2\varphi}{\partial t^2} \tag{17}$$

$$a_{10}\nabla^2\varphi + a_{11}\nabla^2\psi - a_{12} e - a_{13}\varphi - a_{14}\psi + a_{15} T = \frac{\partial^2\psi}{\partial t^2} \tag{18}$$

$$\left(1 + \tau_0\frac{\partial}{\partial t}\right)\left(a_{16}\frac{\partial e}{\partial t} + a_{17}\frac{\partial\varphi}{\partial t} + a_{18}\frac{\partial\psi}{\partial t} + \frac{\partial T}{\partial t}\right) = \nabla^2 T \tag{19}$$

where:

$$a_1 = \frac{b\alpha_1}{\rho c_1^2\kappa_1^2\omega_1^2} \qquad a_2 = \frac{d\alpha_1}{\rho c_1^2\kappa_1^2\omega_1^2} \qquad a_3 = \frac{\beta T_0}{\rho c_1^2} \qquad a_4 = \frac{\alpha}{\kappa_1 c_1^2}$$
$$a_5 = \frac{b_1}{\kappa_1 c_1^2} \qquad a_6 = \frac{b}{\alpha_1} \qquad a_7 = \frac{\alpha_1}{\kappa_1\omega_1^2} \qquad a_8 = \frac{\alpha_3}{\kappa_1\omega_1^2} \qquad a_9 = \frac{\gamma_1 T_0}{\alpha_1}$$
$$a_{10} = \frac{b_1}{\kappa_2 c_1^2} \qquad a_{11} = \frac{\gamma}{\kappa_2 c_1^2} \qquad a_{12} = \frac{d\kappa_1}{\kappa_2\alpha_1} \qquad a_{13} = \frac{\alpha_3}{\kappa_2\omega_1^2} \qquad a_{14} = \frac{\alpha_2}{\kappa_2\omega_1^2}$$
$$a_{15} = \frac{\gamma_2 T_0\kappa_1}{\alpha_1\kappa_2} \qquad a_{16} = \frac{\beta c_1^2}{\rho C^*} \qquad a_{17} = \frac{\gamma_1\alpha_1 c_1^2}{K^*\kappa_1\omega_1^3} \qquad a_{18} = \frac{\gamma_2\alpha_1 c_1^2}{K^*\kappa_1\omega_1^3}$$

4. Initial and boundary conditions

The initial conditions are given by:

$$\begin{array}{llll} u = 0 = \frac{\partial u}{\partial t} & \varphi = 0 = \frac{\partial\varphi}{\partial t} & & \\ \psi = 0 = \frac{\partial\psi}{\partial t} & T = 0 = \frac{\partial T}{\partial t} & \text{at} & t = 0 \end{array} \tag{20}$$

We consider two types of boundary conditions at $r = a$.

4.1. *Mechanical source*

The mechanical boundary conditions are:

$$t_{rr}(a,t) = \begin{cases} 0 & t \le 0 \\ \eta_1\frac{t}{t_0} & 0 < t \le t_0 \\ \eta_1 & t > t_0 \end{cases} \qquad \begin{array}{lll} \sigma_r(a,t) = 0 & \chi_r(a,t) = 0 & T(a,t) = 0 \end{array} \tag{21}$$

where η_1 is constant and t_0 is called the ramping parameter.

4.2. *Thermal source*

The thermal boundary conditions are:

$$t_{rr}(a,t) = 0 \qquad \sigma_r(a,t) = 0 \qquad \chi_r(a,t) = 0$$

$$T(a,t) = \begin{cases} 0 & t \le 0 \\ T_1\frac{t}{t_0} & 0 < t \le t_0 \\ T_1 & t > t_0 \end{cases} \tag{22}$$

where T_1 is constant.

5. Solution in the Laplace transform domain

Applying the Laplace transform defined by:

$$\bar{f}(s) = L[f(t)] = \int_0^\infty f(t)\, e^{-st} dt \tag{23}$$

on the Eqs.(16)–(19) under the initial conitions (20) and after some simplifications, we obtain:

$$\left(\nabla^8 + B_1\nabla^6 + B_2\nabla^4 + B_3\nabla^2 + B_4\right)\left(\bar{e}, \bar{\varphi}, \bar{\psi}, \bar{T}\right) = 0 \tag{24}$$

where: B_1,B_2, B_3, B_4 are given in the appendix I.
The above system of equations can be factorized as:

$$\left\{\left(\nabla^2 - \lambda_1^2\right)\left(\nabla^2 - \lambda_2^2\right)\left(\nabla^2 - \lambda_3^2\right)\left(\nabla^2 - \lambda_4^2\right)\right\}\left(\bar{e}, \bar{\varphi}, \bar{\psi}, \bar{T}\right) = 0 \tag{25}$$

where: λ_1^2, λ_2^2, λ_3^2, λ_4^2 are the roots of the following characteristic equation:

$$\lambda^8 + B_1\lambda^6 + B_2\lambda^4 + B_3\lambda^2 + B_4 = 0 \tag{26}$$

Therefore, the solutions of the Eq. (24), which is bounded at infinity, is given by:

$$\begin{aligned}
\bar{e}(r,s) &= \frac{1}{r}(C_1\exp(-\lambda_1 r) + C_2\exp(-\lambda_2 r) + C_3\exp(-\lambda_3 r) \\
&\quad + C_4\exp(-\lambda_4 r)) && (27)\\
\bar{\varphi}(r,s) &= \frac{1}{r}(g_{11}C_1\exp(-\lambda_1 r) + g_{12}C_2\exp(-\lambda_2 r) + g_{13}C_3\exp(-\lambda_3 r) \\
&\quad + g_{14}C_4\exp(-\lambda_4 r)) && (28)\\
\bar{\psi}(r,s) &= \frac{1}{r}(g_{21}C_1\exp(-\lambda_1 r) + g_{22}C_2\exp(-\lambda_2 r) + g_{23}C_3\exp(-\lambda_3 r) \\
&\quad + g_{24}C_4\exp(-\lambda_4 r)) && (29)\\
\bar{T}(r,s) &= \frac{1}{r}(g_{31}C_1\exp(-\lambda_1 r) + g_{32}C_2\exp(-\lambda_2 r) + g_{33}C_3\exp(-\lambda_3 r) \\
&\quad + g_{34}C_4\exp(-\lambda_4 r)) && (30)
\end{aligned}$$

where: g_{1i}, g_{2i}, g_{3i}, $(i = 1, 2, 3, 4)$ are given in the appendix II.
On solving Eq. (14) with the aid of Eq. (24) and assuming that $u(r,t)$ vanishes at infinity, we obtain:

$$\bar{u}(r,s) = -\frac{1}{r^2}\left[\begin{array}{l} \frac{(\lambda_1 r+1)}{\lambda_1^2}C_1\exp(-\lambda_1 r) + \frac{(\lambda_2 r+1)}{\lambda_2^2}C_2\exp(-\lambda_2 r) \\ +\frac{(\lambda_3 r+1)}{\lambda_3^2}C_3\exp(-\lambda_3 r) + \frac{(\lambda_4 r+1)}{\lambda_4^2}C_4\exp(-\lambda_4 r) \end{array}\right] \tag{31}$$

On using Eqs. (27)–(30) in Eqs. (9), (12), (13) and with the help of Eqs. (15) and (23), we obtain the corresponding expressions for radial stress and equilibrated

stresses as:

$$\begin{aligned}\bar{t}_{rr}(r,s) &= \sum_{i=1}^{4}\left(p_1\left(\frac{\lambda_i^2+2(\lambda_i+1)}{\lambda_i^2}\right)+p_2+p_3g_{1i}\right.\\ &\left.+p_4g_{2i}-g_{3i}\right)C_i(s)\exp(-\lambda_i r) \qquad (32)\\ \bar{\sigma}_r(r,s) &= \sum_{i=1}^{4}\lambda_i(p_5g_{1i}+p_6g_{2i})C_i(s)\exp(-\lambda_i r) \qquad (33)\\ \bar{\chi}_r(r,s) &= \sum_{i=1}^{4}\lambda_i(p_6g_{1i}+p_7g_{2i})C_i(s)\exp(-\lambda_i r) \qquad (34)\end{aligned}$$

where:

$$p_1=\tfrac{2\mu}{\beta T_0} \quad p_2=\tfrac{\lambda}{\beta T_0} \quad p_3=\tfrac{b\alpha_1}{\beta T_0\kappa_1\omega_1^2} \quad p_4=\tfrac{d\alpha_1}{\beta T_0\kappa_1\omega_1^2}$$
$$p_5=\tfrac{\alpha_1}{\kappa_1\omega_1^2} \quad p_6=\tfrac{b_1\alpha_1}{\alpha\kappa_1\omega_1^2} \quad p_7=\tfrac{\gamma\alpha_1}{\alpha\kappa_1\omega_1^2}$$

In Laplace transform domain, the boundary conditions become:

1. Mechanical boundary condition:

$$\bar{t}_{rr}(a,s)=\frac{\eta_1(1-e^{-st_0})}{t_0s^2}=F_1(say)$$

$$\bar{\sigma}_r(a,s)=0 \qquad \bar{\chi}_r(a,s)=0 \qquad \bar{T}(a,s)=0 \qquad (35)$$

2. Thermal boundary condition:

$$\bar{t}_{rr}(a,s)=0 \qquad \bar{\sigma}_r(a,s)=0 \qquad \bar{\chi}_r(a,s)=0$$

$$\bar{T}(a,s)=\frac{T_1(1-e^{-st_0})}{t_0s^2}=F_2(say) \qquad (36)$$

Substituting the values of $\bar{t}_{rr},\bar{\sigma}_r,\bar{\chi}_r$ and $\bar{T}$ from Eqs. (30), (32)–(34) in the boundary conditions (35), (36) yield the corresponding expressions for radial stress, equilibrated stresses and temperature distribution as:

$$\begin{aligned}\bar{t}_{rr}(r,s) &= \frac{1}{\Gamma}(H_{11}\Gamma_1\exp(-\lambda_1 r)+H_{12}\Gamma_2\exp(-\lambda_2 r)+H_{13}\Gamma_3\exp(-\lambda_3 r)\\ &+H_{14}\Gamma_4\exp(-\lambda_4 r)) \qquad (37)\\ \bar{\sigma}_r(r,s) &= \frac{1}{\Gamma}(H_{21}\Gamma_1\exp(-\lambda_1 r)+H_{22}\Gamma_2\exp(-\lambda_2 r)+H_{23}\Gamma_3\exp(-\lambda_3 r)\\ &+H_{24}\Gamma_4\exp(-\lambda_4 r)) \qquad (38)\\ \bar{\chi}_r(r,s) &= \frac{1}{\Gamma}(H_{31}\Gamma_1\exp(-\lambda_1 r)+H_{32}\Gamma_2\exp(-\lambda_2 r)+H_{33}\Gamma_3\exp(-\lambda_3 r)\\ &+H_{34}\Gamma_4\exp(-\lambda_4 r)) \qquad (39)\\ \bar{T}(r,s) &= \frac{1}{\Gamma}(H_{41}\Gamma_1\exp(-\lambda_1 r)+H_{42}\Gamma_2\exp(-\lambda_2 r)+H_{43}\Gamma_3\exp(-\lambda_3 r)\\ &+H_{44}\Gamma_4\exp(-\lambda_4 r)) \qquad (40)\end{aligned}$$

where:

$$\Gamma = \begin{vmatrix} H_{11} & H_{12} & H_{13} & H_{14} \\ H_{21} & H_{22} & H_{23} & H_{24} \\ H_{31} & H_{32} & H_{33} & H_{34} \\ H_{41} & H_{42} & H_{43} & H_{44} \end{vmatrix} \tag{41}$$

Γ_i $(i = 1\,, 2, 3, 4)$ are obtained by replacing i^{th} column of (41) with $[F_1\ 0\ \ 0\ \ F_2\ ]^T$ where: H_{1i}, H_{2i}, H_{3i}, H_{4i}, $(i = 1, 2, 3, 4)$ are given in the appendix II.

Case **4.1.** ***Mechanical source***

If $F_2 = 0$ in Eqs. (37)–(40), yields the resulting expressions for mechanical source.

Case **4.2** ***Thermal source***

If $F_1 = 0$ in Eqs. (37)–(40), we obtain the corresponding expressions for thermal source.

This completes the solution of the problem in Laplace domain.

6. Special cases

Case 6.1: If $b_1 = \alpha_3 = \gamma = \alpha_2 = \gamma_2 = d \to 0$ in Eqs. (37)–(40), we obtain the corresponding expressions for an infinite thermoelastic single porous body with a spherical cavity.

Case 6.2: If $\tau_0 = 0$, in Eqs. (37)–(40) yield the corresponding expressions for an infinite thermoelastic double porous body with a spherical cavity in the context of coupled theory of thermoelasticity.

Case 6.3 : If $\alpha = b = b_1 = \alpha_1 = \alpha_2 = \alpha_3 = \gamma = \gamma_1 = \gamma_2 = d \to 0$ in Eqs. (37)–(40), we obtain the corresponding expressions for an infinite body with a spherical cavity in the theory of thermoelasticity with one relaxation time which is same as obtained by Allam et al. [26] in the absence of magnetic field effect.

7. Inversion of the Laplace domain

In order to invert the Laplace transform, we adopt a numerical inversion method based on a Fourier series expansion [30].

By this method the inverse $f(t)$ of the Laplace transform $\bar{f}(s)$is approximated by:

$$f(t) = \frac{e^{ct}}{t_1}\left[\frac{1}{2}\bar{f}(c) + Re\sum_{k=1}^{N}\bar{f}\left(c + \frac{ik\pi}{t_1}\right)\exp\left(\frac{ik\pi t}{t_1}\right)\right] \qquad 0 < t_1 < 2t$$

where N is sufficiently large integer representing the number of terms in the truncated Fourier series, chosen such that

$$f(t) = \exp(ct)Re\left[\bar{f}\left(c + \frac{iN\pi}{t_1}\right)\exp\left(\frac{iN\pi t}{t_1}\right)\right] \leq \varepsilon_1$$

where $\varepsilon_1$is a prescribed small positive number that corresponds to the degree of accuracy required. The parameter c is a positive free parameter that must be greater than the real part of all the singularities of $\bar{f}(s)$. The optimal choice of c was obtained to the criterion described in expansion [30].

Two methods are used to reduce the total error. First, Korrecktur method is used to reduce the discretization error. Next, the e–algorithm is used to reduce the

truncation eror and hence to accelerate convergence. It should be noted that a good choice of the free parameters N and ct is not only important for the accuracy of the results but also for the application of Korrecktur method and the methods for the acceleration of convergence.

8. Numerical results and discussion

The material chosen for the purpose of numerical computation is copper, whose physical data is given by [31] as:

$$\lambda = 7.76 \times 10^{10} Nm^{-2} \quad C^* = 3.831 \times 10^3 m^2 s^{-2} K^{-1} \quad \mu = 3.86 \times 10^{10} Nm^{-2}$$

$$K^* = 3.86 \times 10^3 Ns^{-1} K^{-1} \; T_0 = 293K \; \alpha_t = 1.78 \times 10^{-5} K^{-1} \; \rho = 8.954 \times 10^3 Kgm^{-3}$$

The double porous parameters are taken as:

$$\alpha_2 = 2.4 \times 10^{10} Nm^{-2} \qquad \alpha_3 = 2.5 \times 10^{10} Nm^{-2} \qquad \gamma = 1.1 \times 10^{-5} N$$

$$\alpha = 1.3 \times 10^{-5} \; N \qquad \gamma_1 = 0.16 \times 10^5 Nm^{-2} \qquad b_1 = 0.12 \times 10^{-5} \; N$$

$$d = 0.1 \times 10^{10} Nm^{-2} \qquad \gamma_2 = 0.219 \times 10^5 Nm^{-2} \qquad \kappa_1 = 0.1456 \times 10^{-12} Nm^{-2} s^2$$

$$b = 0.9 \times 10^{10} Nm^{-2} \qquad \alpha_1 = 2.3 \times 10^{10} \; Nm^{-2} \qquad \kappa_2 = 0.1546 \times 10^{-12} Nm^{-2} s^2$$

The software MATLAB has been used to find the values of radial stress t_{rr}, hoop stress $t_{\vartheta\vartheta}$, equilibrated stresses σ_r, χ_r and temperature distribution T. The variations of these values with respect to radial distance r have been shown in Figs. 1–20 in case of mechanical and thermal source. In Figs. 1–10, effect of porosity is shown graphically for time $t = 0.1$, 0.5. In these figures, solid lines without and with central symbols correspond to Lord–Shulman (LS) theory of thermoelasticity for $t = 0.1, 0.5$ respectively and small dashed line without and with central symbols correspond to coupled theory (CT)of thermoelasticity for $t = 0.1, 0.5$ respectively. Also, the effect of porosity is depicted graphically in Figs. 11–20. In Figs. 11–20, solid lines without and with central symbols correspond to thermal double porous material (TDP) for $t = 0.1$, 0.5 respectively and small dashed line without and with central symbols correspond to thermal single porous material (TSP) for $t = 0.1$, 0.5 respectively. The computations were carried out for $t_0 = 0.2$, $\eta_1 = 1$, $T_1 = 1$

8.1. *Effect of thermal relaxation time*

8.1.1. *Mechanical source*

From Fig. 1 and 2, it is noticed that the trend and behavior of variation of t_{rr} and $t_{\vartheta\vartheta}$are similar for both LS and CT theories of thermoelasticity. The value decreases for the region $r \leq 2$ and increases further with increase in r. It is found that the relaxation time decreases the values of stresses for LS theory in comparison to CT theory. The values of t_{rr} and $t_{\vartheta\vartheta}$ also increase with the increase in time. Figs. 3 and 4 show that the values of σ_r and χ_r increase for $1 < r \leq 2$, decrease for $2 < r \leq 3.5$ and become almost stationary as $r > 3.5$. The behavior of variation is same for both LS and CT theories of thermoelasticity.

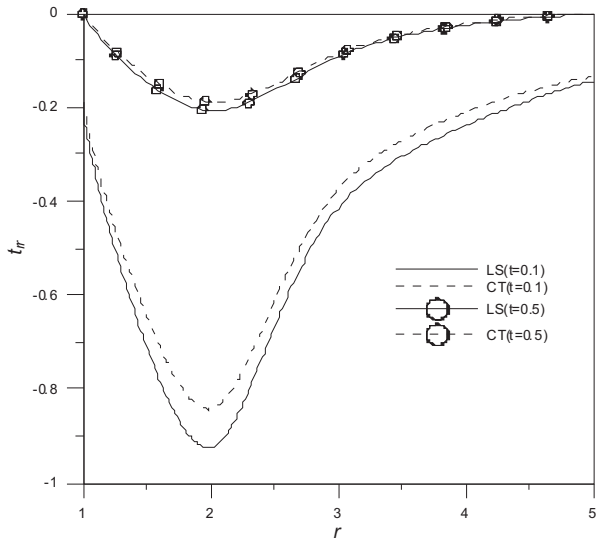

Figure 1 Variation of radial stress t_{rr} w.r.t. radial distance r (Mechanical source)

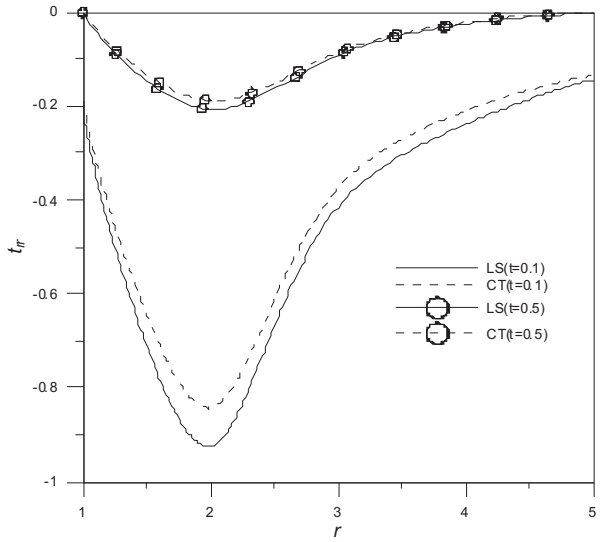

Figure 2 Variation of hoop stress $t_{\vartheta\vartheta}$ w.r.t. radial distance r (Mechanical source)

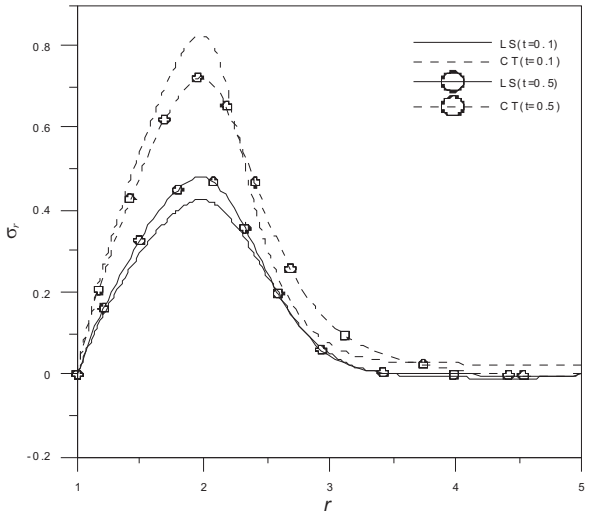

Figure 3 Variation of equilibrated stress σ_r w.r.t. radial distance r (Mechanical source)

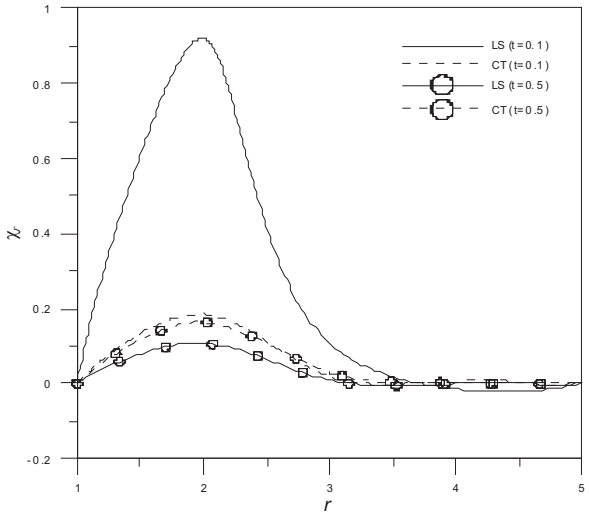

Figure 4 Variation of equilibrated stress χ_r w.r.t. radial distance r (Mechanical source)

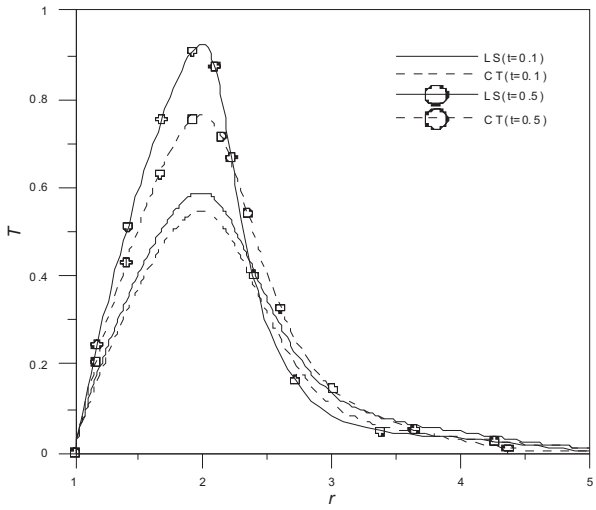

Figure 5 Variation of temperature distribution T w.r.t. radial distance r (Mechanical source)

It is clear from the figures that for σ_r, the values are more for CT theory as compared to the values of LS theory while incase of χ_r, an opposite behavior is noticed. Also, the values are not necessarily increase with the increase in time t. Fig. 5 depicts that, the value of T increases for the region $r \leq 2$ and then decreases onwards. The values are more for LS theory due to the effect of relaxation time. It is also found that the value of T increases with the increase in time t.

8.1.2. *Thermal source*

Fig. 6 represents the value of t_{rr} decrease for $r \leq 2$ and become stationary onwards for LS theory while for CT theory of thermoelasticity, it decreases for $r \leq 2$ and then increases in the remaining region. It is also found the due to relaxation time, the values are more for LS theory. With increase in time, the value of t_{rr} also increases for both the theories. Fig. 7 shows the value of $t_{\vartheta\vartheta}$ decrease for $r \leq 2$ and become almost stationary for the subsequent region incase of LS theory. For CT theory of thermoelasticity, it decreases for $r \leq 2$, increases for $2 < r \leq 3$ and decreases onwards. Due to effect of relaxation time, the values are smaller for LS theory in comparison to CT theory at $t = 0.1$ while an opposite trend is noticed at $t = 0.5$. Figs. 8 and 9 show that the values of σ_r and χ_r decrease for $1 < r < 3$, increase for $3 < r < 4$ and again start decreasing as $r \geq 4$, for both the theories at $t = 0.1$. For $t = 0.5$, it decrease for $1 < r \leq 2$, increase for $2 < r \leq 3$ and become almost stationary as $r > 3$, for both the theories of thermoelasticity. The values remain

more in case of CT theory except for the region for $r \geq 3.5$ where the behavior gets reversed. The values of stresses may not necessarily increase with the increase in time t. From Fig. 10, it is evident that the value of T increases for the region $r \leq 2$ and then decreases further for both the theories and for both the values of time t. Relaxation time increases the value of T for LS theory in comparison to the values for CT theory. It is also noticed that as t increases, the value of T decreases.

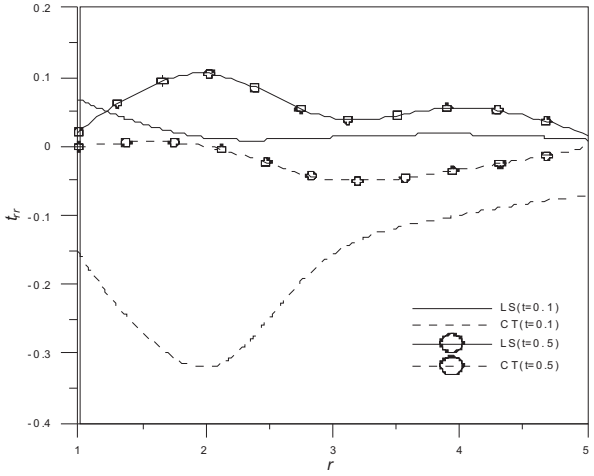

Figure 6 Variation of radial stress t_{rr} w.r.t. radial distance r (Thermal source)

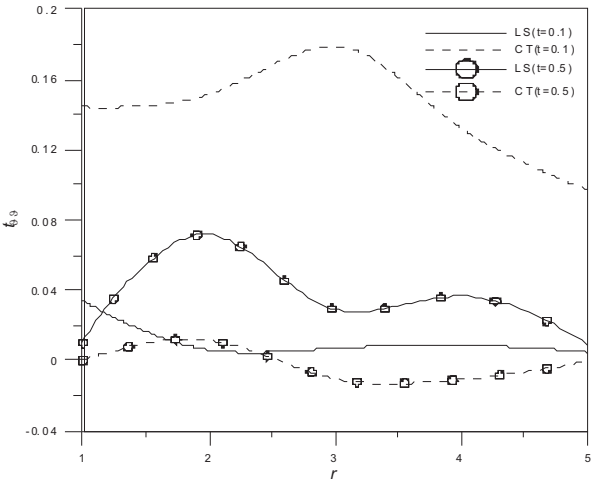

Figure 7 Variation of hoop stress $t_{\vartheta\vartheta}$ w.r.t. radial distance r (Thermal source)

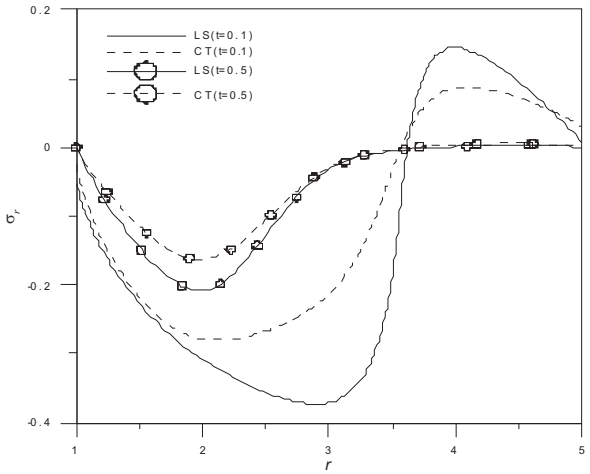

Figure 8 Variation of equilibrated stress σ_r w.r.t. radial distance r (Thermal source)

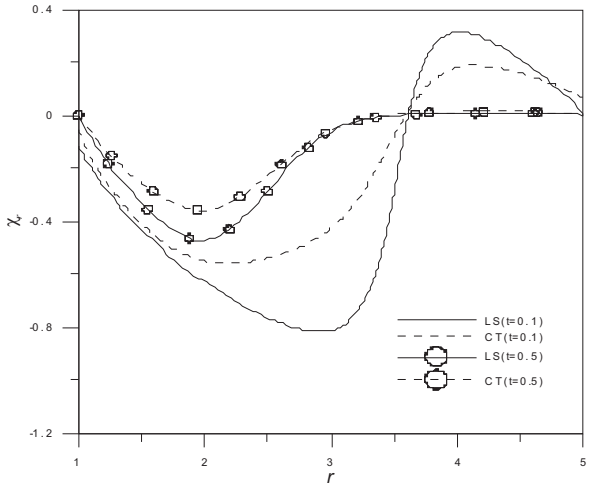

Figure 9 Variation of equilibrated stress χ_r w.r.t. radial distance r (Thermal source)

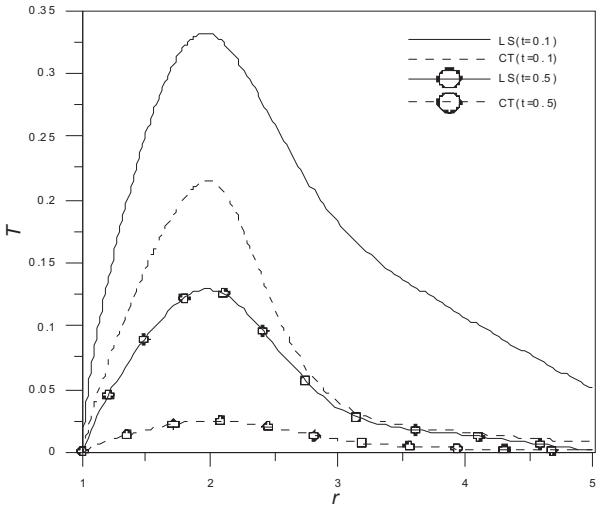

Figure 10 Variation of temperature distribution T w.r.t. radial distance r (Thermal source)

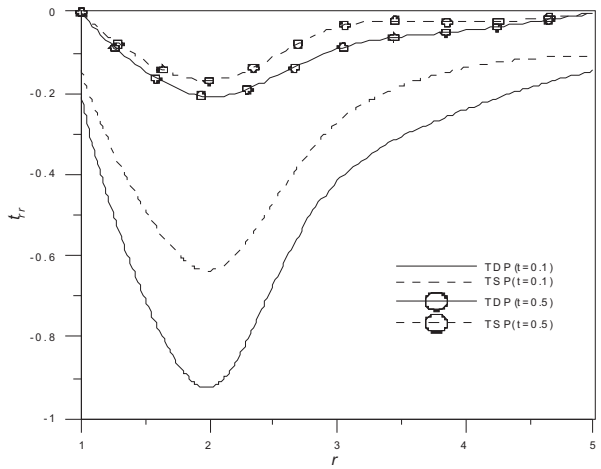

Figure 11 Variation of radial stress t_{rr} w.r.t. radial distance r (Mechanical source)

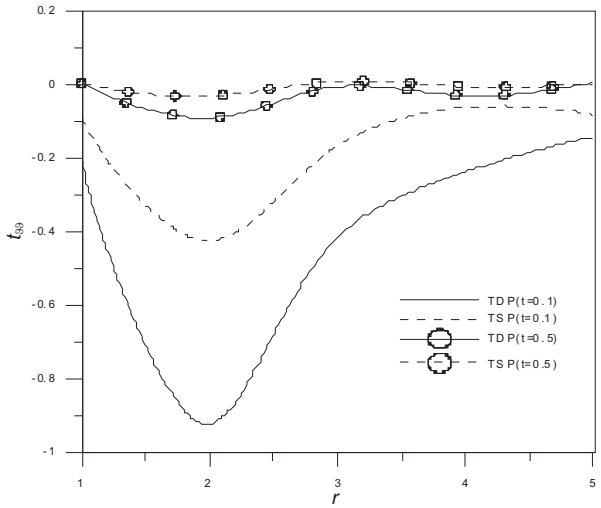

Figure 12 Variation of hoop stress $t_{\vartheta\vartheta}$ w.r.t. radial distance r (Mechanical source)

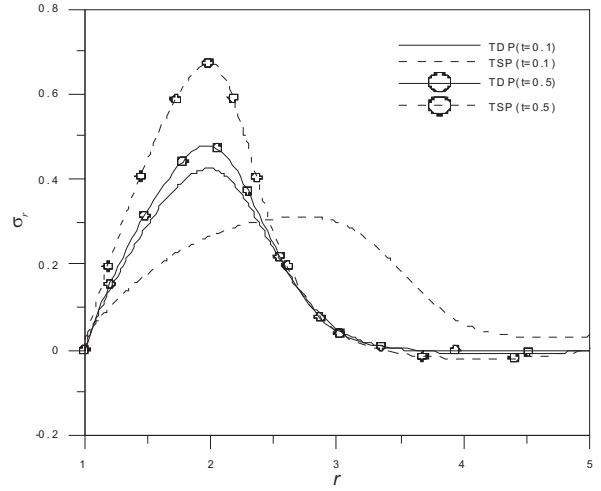

Figure 13 Variation of equilibrated stress σ_r w.r.t. radial distance r (Mechanical source)

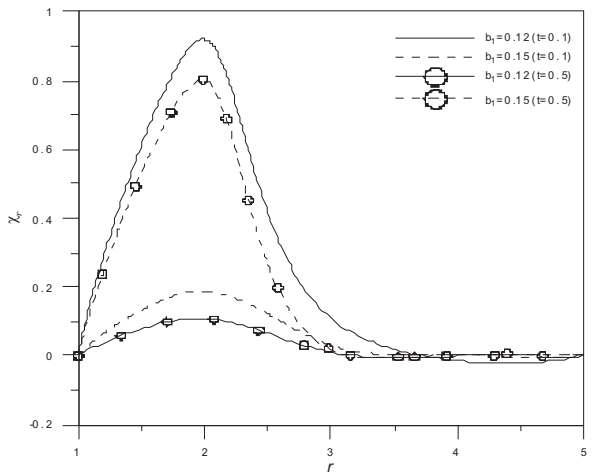

Figure 14 Variation of equilibrated stress χ_r w.r.t. radial distance r (Mechanical source)

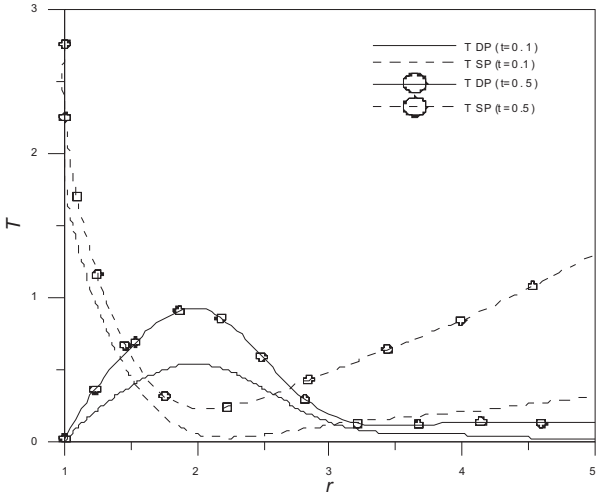

Figure 15 Variation of temperature distribution T w.r.t.radial distance r (Mechanical source)

8.2. *Effect of porosity*

8.2.1. *Mechanical source*

Figs. 11 and 12, depict that the trend and behavior of variation of t_{rr} and $t_{\vartheta\vartheta}$ are similar for both TDP and TSP for both values of time t. The value of t_{rr} and $t_{\vartheta\vartheta}$ decrease for $r \leq 2$ and increases further as $r$increases.The values of stresses

are more for TSP as compared to the values for TDP due to effect of porosity. It is also found that the values of stresses increase with increase in value of time$t$. Fig. 13 represents that the value of σ_r is higher near the boundary surface of the cavity and decreases with increase in r.The magnitude values of σ_r are more for TDP for the region $1 < r \leq 2.5$, while an opposite trend is noticed in the remaining region, at $t = 0.1$. The value of TSP remain higher than that of TDP for all r, at $t = 0.5$. Fig. 14 shows that the value of χ_r increases for the region $1 < r \leq 2$ and deceases onwards as r increases. At $t = 0.1$, the magnitude values of χ_r decreases with the increase in porous parameter b_1 while an opposite trend is noticed at $t = 0.5$. From Fig. 15, it is clear that the trend and behavior of variation is opposite for TDP and TSP. The magnitude value of T also increases with the increase in time t.

8.2.2. *Thermal source*

Figs. 16 and 17 show that, the magnitude values of t_{rr} and $t_{\vartheta\vartheta}$ are more for TDP in comparison to TSP due to effect of porosity. The values of t_{rr} and $t_{\vartheta\vartheta}$ also get increased as t increases except for $1 < r \leq 1.5$ where an opposite trend of variation is noticed. From Fig. 18, it is clear that the magnitude values of σ_r is higher for TSP as compared to that of TDP for the region $1 < r \leq 3.5$, while the behavior gets reversed in the subsequent region. As t increases, the magnitude value of σ_r also increases near the surface of the cavity. Fig. 19 depicts that the magnitude values of χ_r increases with the increase in porous parameter b_1 for $1 < r \leq 3.5$ while an opposite behavior is noticed in the remaining region. From fig. 20, it is evident that an opposite trend and behavior of variation is shown for TDP and TSP. The magnitude value of T are more for TSP than that of values of TDP, near the boundary of the cavity. The values of T may not necessarily increase with the increase in time t.

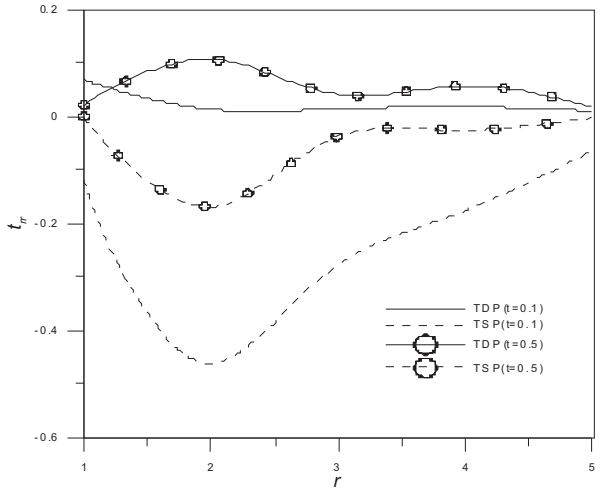

Figure 16 Variation of radial stress t_{rr} w.r.t. radial distance r (Thermal source)

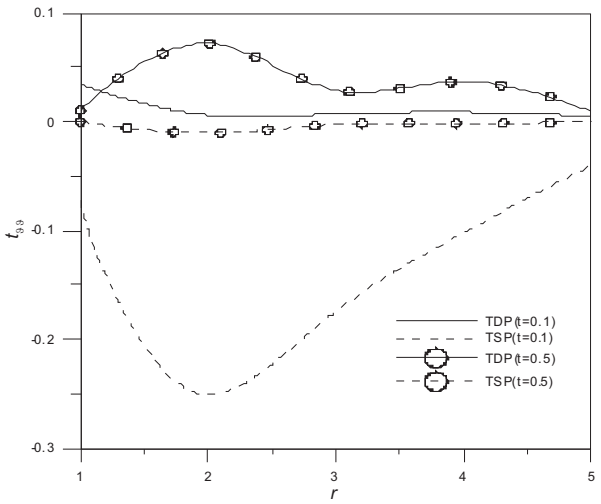

Figure 17 Variation of hoop stress $t_{\vartheta\vartheta}$ w.r.t. radial distance r (Thermal source)

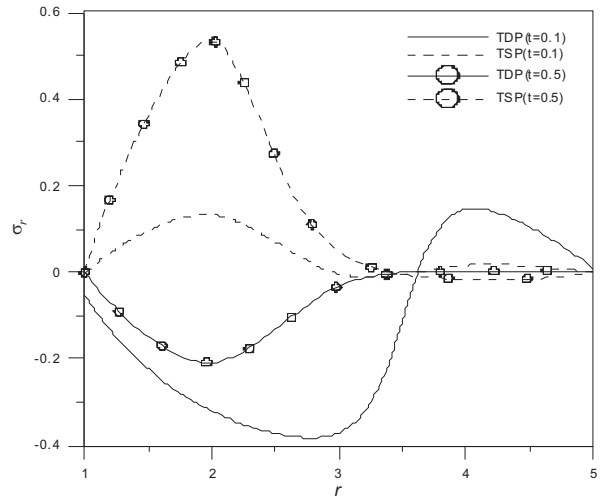

Figure 18 Variation of equilibrated stress σ_r w.r.t. radial distance r (Thermal source)

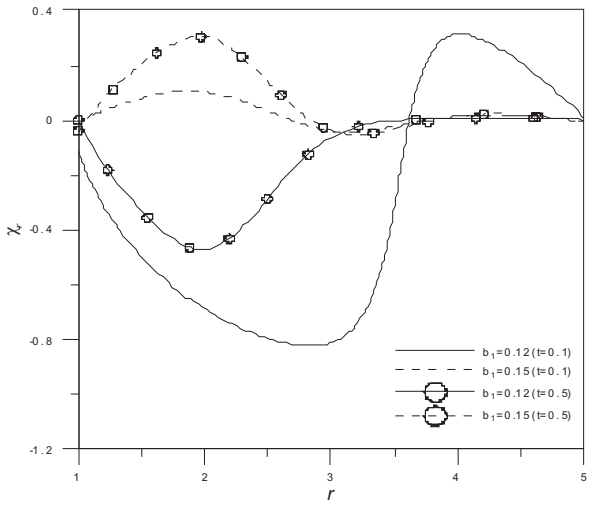

Figure 19 Variation of equilibrated stress χ_r w.r.t. radial distance r (Thermal source)

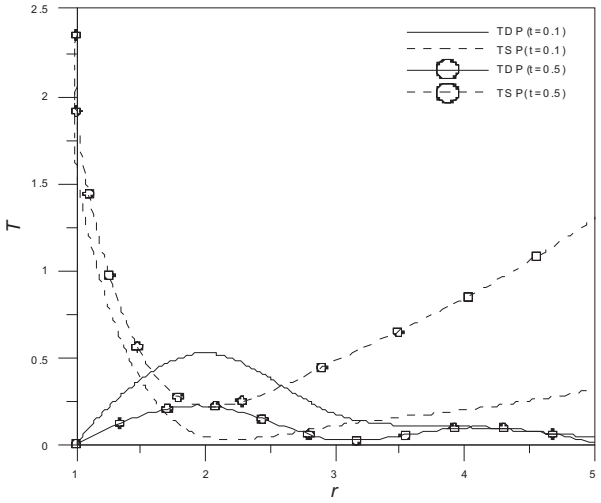

Figure 20 Variation of temperature distribution T w.r.t radial distance r (Thermal source)

9. Concluding remarks

In this paper, we have examined the elastodynamic problem of an infinite thermoelastic double porous body with a spherical cavity in the context of Lord-Shulman theory of thermoelasticity with one relaxation time subjected to ramp type mechanical/thermal source. Due to the complicated nature of the governing equations of thermoelasticity theory with double porosity structure, limited work has been done

in this field. Analysis of elastodynamics deformation in thermoelastic materials due to mechanical/thermal source is a significant problem of mechanics.

It is concluded that the variation in the stress components and temperature distribution is more near the boundary surface of the spherical cavity. All the field quantities are observed to be very sensitive towards the porosity and thermal relaxation time parameters. From figures, it is evident that porosity effect plays an important role. Graphical representation indicated that double porosity and single porosity have both the increasing and decreasing effects on the numerical values of the physical quantities. Thermal relaxation parameter also has a significant effect on all the physical quantities which shows that it is very important to take into account the relaxation time parameter.

This type of study is useful due to its application in geophysics and rock mechanics. The results obtained in this investigation should prove to be beneficial for the researchers working on the theory of thermoelasticity with double porosity structure. The introduction of double porous parameter to the thermoelastic medium represents a more realistic model for further studies.

References

[1] **Lord, H. and Shulman, Y.:** A generalized dynamical theory of thermoelasticity, *J. Mech. Phys. Solids*, 15, 299–309, **1967**.

[2] **Biot, M. A.:** General theory of three–dimensional consolidation, *J. Appl. Phys.,* 12, 155–164, **1941**.

[3] **Barenblatt, G.I., Zheltov, I.P. and Kochina, I. N.:** Basic concept in the theory of seepage of homogeneous liquids in fissured rocks (strata), *J. Appl. Math. Mech.,* 24, 1286-1303, **1960**.

[4] **Aifantis, E. C.:** Introducing a multi–porous medium, *Developments in Mechanics*, 8, 209–211, **1977**.

[5] **Aifantis, E. C.:** On the response of fissured rocks, *Developments in Mechanics*, 10, 249–253, **1979**.

[6] **Aifantis, E. C.:** The mechanics of diffusion in solids, T.A.M. Report No. 440, *Dept. of Theor. Appl. Mech., University of Illinois*, Urbana, Illinois, **1980.**

[7] **Aifantis, E. C.:** On the Problem of Diffusion in Solids, *Acta Mech.*, 37, 265–296, **1980.**

[8] **Wilson, R. K. and Aifantis, E. C.:** On the theory of consolidation with double porosity, *Int. J. Engg. Sci.,* 20, No.9, 1009-1035, **1984**.

[9] **Khaled, M. Y., Beskos, D. E. and Aifantis, E. C.:** On the theory of consolidation with double porosity-III, *Int. J. Numer. Analy. Meth. Geomech.* 8, 101–123, **1984**.

[10] **Wilson, R. K. and Aifantis, E. C.:** A double porosity model for acoustic wave propagation in fractured porous rock. *Int. J. Engg. Sci.*, 22, (8–10), 1209–1227, **1984**.

[11] **Nunziato , J.W. and Cowin , S.C.:** A nonlinear theory of elastic materials with voids. *Arch. Rat. Mech. Anal.,* 72 , 175-201, **1979**.

[12] **Cowin, S.C. and Nunziato, J. W.:** Linear elastic materials with voids, *J. Elasticity*, 13, 125-147, **1983**.

[13] **Beskos, D. E. and Aifantis, E. C.:** On the theory of consolidation with Double Porosity-II, *Int. J. Engg. Sci.*, 24, 1697-1716, **1986.**

[14] **Khalili, N. and Valliappan, S.:** Unified theory of flow and deformation in double porous media. *Eur. J. Mech. A, Solids*, 15 , 321-336, **1996**.

[15] **Khalili, N. and Selvadurai, A. P. S.:** A Fully Coupled Constitutive Model for Thermo-hydro –mechanical Analysis in Elastic Media with Double Porosity, *Geophys. Res. Lett.,* 30 , 2268-2271, **2003**.

[16] **Svanadze, M.:** Fundamental solution in the theory of consolidation with double porosity, *J. Mech. Behav. Mater.* , 16 , 123-130, **2005**.

[17] **Svanadze, M.:** Dynamical problems on the theory of elasticity for solids with double porosity, *Proc. Appl. Math. Mech.* 10, 209-310, **2010**.

[18] **Svanadze, M.:** Plane waves and boundary value problems in the theory of elasticity for solids with double porosity. *Acta Appl. Math.,* 122, 461-470, **2012**.

[19] **Straughan, B.:** Stability and uniqueness in double porosity elasticity, *Int. J. Eng. Sci.*, 65, 1-8, **2013**.

[20] **Svanadze, M.:** On the theory of viscoelasticity for materials with double porosity, *Disc. and Cont. Dynam. Syst. Ser. B.,* 19 No.7, 2335-2352, **2014**.

[21] **Svanadze, M.:** Uniqueness theorems in the theory of thermoelasticity for solids with double porosity, *Meccanica*, 49 , 2099–2108, **2014**.

[22] **Iesan, D. and Quintanilla, R.:** On a theory of thermoelastic materials with a double porosity structure, *J. Therm. Stress.,* 37, 1017–1036, **2014**.

[23] **Allam, M. N. Elsibai, K. A. and Abouelergal, A. E.:** Thermal stresses in a harmonic field for an infinite body with a circular cylindrical hole without energy dissipation, *J. Therm. Stresses,* 25, 57–68, **2002**.

[24] **Youssef, H. M.:** Generalized thermoelasticity of an infinite body with a cylindrical cavity and variable material properties, *J. Therm. Stresses*, 28, 521–532, **2005**.

[25] **Youssef, H. M.:** State space approach on generalized thermoelasticity for an infinite material with a spherical cavity and variable thermal conductivity subjected to ramp–type heating, *Canadian Applied Mathematics Quarterly, 13,* No.4 , 369–390, **2005**.

[26] **Allam, M. N, Elsibai, K.A. and Abouelregal, A.E.:** Magneto-thermoelasticity for an infinite body with a spherical cavity and variable material properties without energy dissipation, *Int. J. Solids Struct.*, 47, 2631–2638, **2010**.

[27] **Abd-alla, A. M. and Abo-dahab, S. M.:** Effect of rotation and initial stress on an infinite generalized magneto-thermoelastic diffusion body with a spherical cavity, *J. of Thermal Stresses,* 35, 892–912, **2012.**

[28] **Zenkour, A. M. and Abouelregal, A. E.:** Effects of phase-lags in a thermoviscoelastic orthotropic continuum with a cylindrical hole and variable thermal conductivity, *Arch. Mech.,* 67, No.6, 457–475, **2015**.

[29] **Abbas, I. A., Kumar, R. and Rani, L.:** Thermoelastic interaction in a thermally conducting cubic crystal subjected to ramp-type heating, *Appl. Math.Comp.* 254, 360–369, **2015**.

[30] **Honig, G. and Hirdes, U.:** A method for the numerical inversion of the Laplace transforms, *J. Comp. Appl. Math.*, 10, 113–132, **1984**.

[31] **Sherief, H. and Saleh, H.:** A half space problem in the theory of generalized thermoelastic diffusion, *Int. J. Solid. Struct.*, 42, 4484–4493, **2005**.

[32] **Khalili, N.:** Coupling effects in double porosity media with deformable matrix, *Geophys. Res. Lett.,* 30, 22 , DOI 10.1029/2003GL018544, **2003**.

Appendix I

$a_{19} = s(1+\tau_0 s) \quad a_{20} = s(1+\tau_0 s)a_{16} \quad a_{21} = s(1+\tau_0 s)a_{17} \quad a_{22} = s(1+\tau_0 s)a_{18}$
$n_1 = -\left(a_7 + s^2\right) \quad n_2 = -\left(a_{14} + s^2\right) \quad r_1 = a_5 a_{10} - a_4 a_{11}$
$r_2 = a_4(a_{11}a_{19} - n_2) - a_{11}n_1 - a_7 a_{10} - a_5(a_{10}a_{19} + a_{13})$
$r_3 = n_1(a_{11}a_{19} - n_2) + a_4(n_2 a_{19} - a_{15}a_{22}) + a_5(a_{13}a_{19} + a_{15}a_{21})$
$+a_7(a_{10}a_{19} + a_{13}) + a_9(a_{10}a_{22} - a_{11}a_{21}),$
$r_4 = n_1(n_2 a_{19} - a_{15}a_{22}) - a_8(a_{13}a_{23} + a_{15}a_{21}) - a_9(a_{13}a_{22} + n_2 a_{21})$
$r_5 = a_6 a_{11} - a_5 a_{12},$
$r_6 = -a_6(a_{11}a_{19} - n_2) + a_7 a_{12} + a_5(a_{19}a_{12} + a_{15}a_{20}) - a_9 a_{11}a_{20}$
$r_7 = -a_6(n_2 a_{19} - a_{15}a_{22}) - a_7(a_{12}a_{19} + a_{15}a_{20}) - a_8(a_{12}a_{22} + n_2 a_{20})$
$r_8 = a_6 a_{10} - a_4 a_{12}, r_9 = -a_6(a_{13} + a_{10}a_{19}) - n_1 a_{12} + a_4(a_{12}a_{19} + a_{15}a_{20})$
$r_{10} = a_9(a_{13}a_{20} - a_{12}a_{21}) + n_1(a_{12}a_{19} + a_{15}a_{20}) + a_6\,(a_{13}a_{19} + a_{15}a_{21})$
$r_{11} = a_{20}(a_4 a_{11} - a_5 a_{10})$
$r_{12} = a_6(a_{11}a_{21} - a_{10}a_{22}) + a_{20}(n_1 a_{11} + a_7 a_{10})$
$+a_4(a_{12}a_{22} + n_2 a_{20}) + a_5(a_{13}a_{20} - a_{12}a_{21})$
$r_{13} = a_7(a_{12}a_{21} - a_{13}a_{20}) + a_6(a_{13}a_{22} + n_2 a_{21}) + n_1(a_{12}a_{22} + n_2 a_{20})$
$B_1 = \left(r_2 - s^2 r_1\right)/r_1$
$B_2 = \left(r_3 - s^2 r_2 - a_1 r_5 + a_2 r_8 + a_3 r_{11}\right)/r_1$
$B_3 = \left(r_4 - s^2 r_3 - a_1 r_6 + a_2 r_9 + a_3 r_{12}\right)/r_1$
$B_4 = \left(-s^2 r_4 - a_1 r_7 + a_2 r_{10} + a_3 r_{13}\right)/r_1$

Appendix II

$g_{1i} = -\left\{r_5\lambda_i^4 + r_6\lambda_i^2 + r_7\right\}/\left\{r_1\lambda_i^6 + r_2\lambda_i^4 + r_3\lambda_i^2 + r_4\right\}$
$g_{2i} = \left\{r_8\lambda_i^4 + r_9\lambda_i^2 + r_{10}\right\}/\left\{r_1\lambda_i^6 + r_2\lambda_i^4 + r_3\lambda_i^2 + r_4\right\}$
$g_{3i} = -\left\{r_{11}\lambda_i^4 + r_{12}\lambda_i^2 + r_{13}\right\}/\left\{r_1\lambda_i^6 + r_2\lambda_i^4 + r_3\lambda_i^2 + r_4\right\} \qquad i = 1,2,3,4$
$H_{11} = p_1\left(\frac{\lambda_1^2 + 2(\lambda_1+1)}{\lambda_1^2}\right) + p_2 + p_3 g_{11} + p_4 g_{21} - g_{31}$
$H_{12} = p_1\left(\frac{\lambda_2^2 + 2(\lambda_2+1)}{\lambda_2^2}\right) + p_2 + p_3 g_{12} + p_4 g_{22} - g_{32}$
$H_{13} = p_1\left(\frac{\lambda_3^2 + 2(\lambda_3+1)}{\lambda_3^2}\right) + p_2 + p_3 g_{13} + p_4 g_{23} - g_{33}$
$H_{14} = p_1\left(\frac{\lambda_4^2 + 2(\lambda_4+1)}{\lambda_4^2}\right) + p_2 + p_3 g_{14} + p_4 g_{24} - g_{34}$
$H_{21} = \lambda_1(p_5 g_{11} + p_6 g_{21})$
$H_{22} = \lambda_2(p_5 g_{12} + p_6 g_{22})$
$H_{23} = \lambda_3(p_5 g_{13} + p_6 g_{23})$
$H_{24} = \lambda_4(p_5 g_{14} + p_6 g_{24})$
$H_{31} = \lambda_1(p_6 g_{11} + p_7 g_{21})$
$H_{32} = \lambda_2(p_6 g_{12} + p_7 g_{22})$
$H_{33} = \lambda_3(p_6 g_{13} + p_7 g_{23})$
$H_{34} = \lambda_4(p_6 g_{14} + p_7 g_{24})$
$H_{41} = g_{31} \qquad H_{42} = g_{32} \qquad H_{43} = g_{33} \qquad H_{44} = g_{34}$